International Standard Problem No. 43: Results and Lessons Learned

Mirela Gavrilas
United States Nuclear Regulatory Commission, Office of Nuclear Regulatory Research

Abstract

In 1997, OECD/CSNI approved testing the mixing associated with inadvertent injection of a boron-dilute slug in a PWR primary system as International Standard Problem No. 43. The tests were performed in the UM 2x4 Loop, a reduced-height, reduced-pressure scale model of the TMI 2 reactor system. The experimental program consisted of four test series, which increased in realism from separate effect to integral facility. Participants collaborated with the UM 2x4 Loop staff in establishing key aspects of the experiment such as figures of merit and the simulation boundary. The facility description included CAD drawings of the system. The nominal test of series A was repeated 18 times to establish an experimental uncertainty band. It became clear that, while these tests agreed with respect to the global figure of merit, the flow patterns fell in two distinct groups. Small variations in initial/boundary conditions caused a change in Fr number that induced the different flow patterns.

Introduction

The use of computational fluid dynamics (CFD) codes in nuclear safety applications has increased significantly over that past decade. With it, the need for specific assessments has increased. Nuclear safety inquiries have specialized assessment needs, which require specialized experimental programs. The industry has substantial experience in conducting both separate effects and integral test experimental programs. This experience was augmented with techniques devised specifically for CFD code verification. An example of a specialized inquiry for nuclear safety is the mixing behaviour of boric acid solution in the reactor vessel of a pressurized water reactor (PWR).

Rapid boron-dilution (RBD) transients have been the subject of investigation for nearly two decades. B-10—a large cross section neutron absorber—is part of routine reactivity control in PWRs. Furthermore, emergency safety systems are designed to decrease core reactivity under accident conditions by injecting soluble boric acid (H_3BO_3) from accumulators and refueling water storage tanks. RBD transients involve the sudden deboration of reactor coolant passing through the core. This resulting reactivity excursion depends on the concentration of poison remaining in the coolant, and its spatial and temporal distribution.

In 1997, the Committee for the Safety of Nuclear Installations (CSNI) within the Organization for Economic Cooperation and Development (OECD) approved an international standard problem (ISP) on the topic of boron dilution. The ISP program began in 1976 and covers multiple technical areas including thermal-hydraulics, behaviour of fuel under high-temperature-transient conditions, hydrogen distribution in containment and seismic behaviour of reactor buildings. The intent of an ISP is fully consistent with the formal definition of validation as stated in AIAA G-077-1998: "The process of determining the degree to which a model is an accurate representation of the real world from the perspective of the intended uses of the model." [1] The intent shapes both the experimental and computational part of the program. The experiment has to be true to the phenomena being investigated, which means that similarity to the prototype has to be considered. The computation has to test not just code models but also the user's competence. This is often accomplished through blind exercises, i.e., exercises in which the user is not given the experimental data until he/she has submitted their simulation. ISP 43 contained a blind exercise test series.

CSNI approved the experimental program to be performed at the University of Maryland 2x4 Thermal-hydraulic Loop (UM 2x4 Loop). A rough outline of the experimental program was presented to CSNI. As various entities began to express interest in participating, it became clear that the codes of choice were going to be CFD codes. This became the first instance of testing CFD codes in an ISP. It was possible to devise the details of the experimental program, including the instrumentation, to make it most useful for CFD code testing. Special consideration was given to setting the requisite tolerances on initial and boundary conditions as well as placing instrumentation such that it is least disturbing to the flow field.

Four test series were performed that sequentially increased realism. The first test series, which became the blind part of the exercise, was nearly a separate effect type experiment. The deborated slug was injected through a single cold leg. The next three test series allowed participation from increasingly more cold legs until all four were involved.

The participants were involved to a large extent in nearly all phases of ISP 43. Specifically, they contributed to the design of the experiments, the decision regarding the figures of merit and the evaluation of test results. This was the principal reason for the success of the program. In this context, success refers to both operational aspects as well as the quality of the submitted simulations.

Experimental Program

In the wider context of code verification and validation (V&V), the stages of experimental testing include unit problems focused on a single phenomenon, benchmark experiments with few coupled phenomena, and subsystem and complete system tests that capture most of the prototype's behavior. In the nuclear industry, the preferred nomenclature has been separate effect and integral testing. Separate effects generally include few phenomena with tightly controlled initial and boundary conditions. Integral tests are designed to capture all of the prototype's key phenomena as well as all relevant interactions. In such a complex system, uncertainties associated with initial and boundary conditions are usually large.

The UM 2x4 Loop was designed as an integral test facility to study thermal-hydraulic processes encountered in the TMI-2 reactor. The facility was a 1/5 scale model of the prototype Babcock and Wilcox (B&W) plant. It was reduced height and scaled 1/500 by volume. Its modular design made it possible to customize both test conditions and the instrumentation to a nearly separate effects configuration for the first test series. Figure 1 shows lateral- and top-view schematics of the facility.

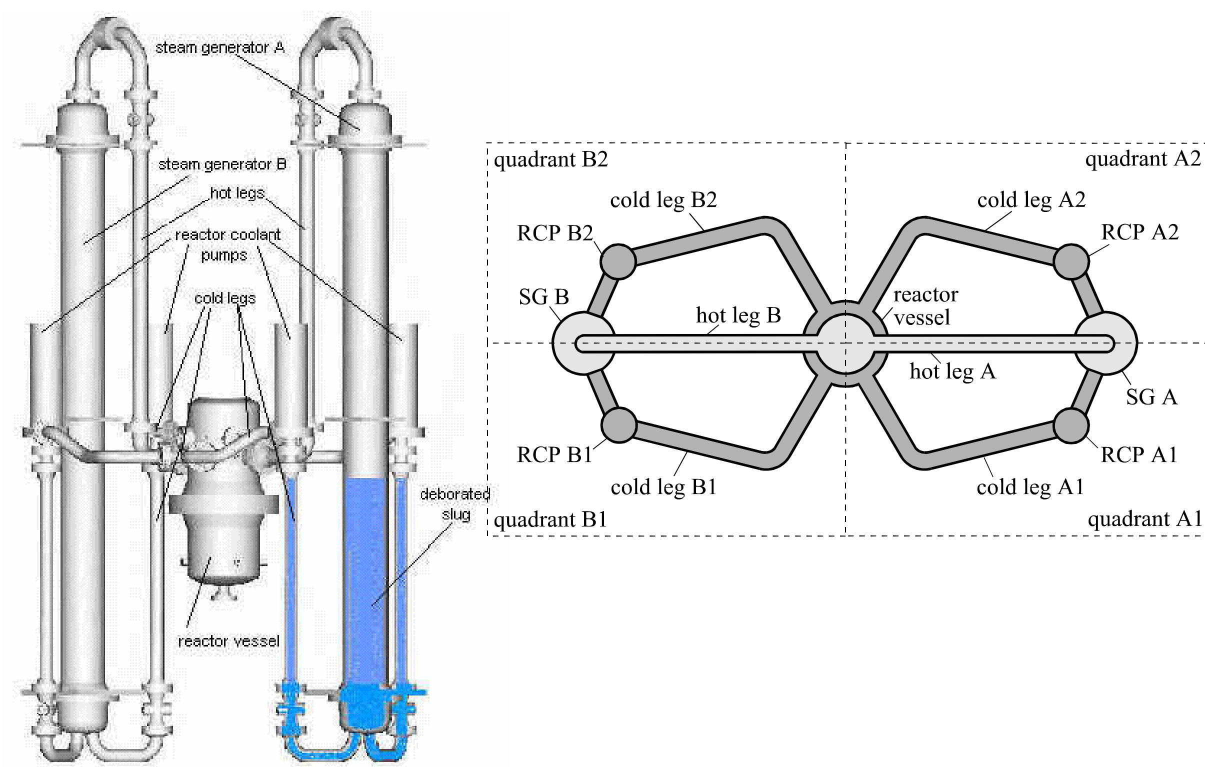

Figure 1. Lateral- and top-view schematic of the UM 2x4 Loop

Note that a CAD program generated the schematics in the above figure. All participating segments of the 2x4 Loop were captured as CAD drawings. The particular CAD program interfaced with both FLUENT and CFX, as well as other codes used by participants. The staff conducting the experiments had a running FLUENT model of the facility that was used to debug the CAD files. The CAD facility model helped ensure geometric data sufficiency and saved those participants who chose to use it a significant amount of time.

The facility was largely similar to a B&W lowered-loop design. The volumetric characteristics are listed in Table 1. The reactor vessel and the instrumentation are depicted in Figure 2. The vessel was made of stainless steel. It was 1.2764 m (50.25 in) in height and had an outside diameter of 0.5080 m (20 in). The wall thickness was 0.0127 m (0.5 in). The core barrel was made of 304 stainless steel with a wall thickness of 0.0048 m (3/16 in). The outer diameter of the core barrel in its upper section was 0.4191 m (16.5 in) and the core barrel outer diameter in its lower section was 0.3810 m (15 in). Thus, the downcomer gap was equal to 0.0508 m (2 in) in the lower portion of the downcomer. In the upper portion, the downcomer gap was 0.0318 m (1.25 in). The wider area in the downcomer corresponds to the smaller diameter of the core barrel and was designed to increase the fractional volume of the downcomer in order to meet the prototypical value. Theses characteristics render the vessel similar to most operating PWRs. Two features that impact mixing and differ from most of the operating PWRs are: the backwards-facing step in the downcomer and the absence of obstructions in the lower plenum.

Table 1.Volumetric characteristics of the 2x4 Loop Facility

System Components	2x4 Loop Facility		TMI-2 Prototype		Ratio (Model to Prototype)
	Volume (l)	Fraction	Volume (l)	Fraction	
Cold legs	77	0.129	41,000	0.136	1: 1.054
Downcomer	55	0.092	28,300	0.094	1: 1.022
Lower plenum	33	0.056	17,600	0.058	1: 1.036
Core	55	0.093	22,100	0.073	1: 0.785
Upper plenum	50	0.084	30,900	0.102	1: 1.214
Upper head	35	0.059	15,600	0.052	1: 0.881

The reboration of the slug was simulated through the thermal mixing of a cold slug into a hot downcomer. Test matrices were devised to measure the extent of mixing for different Re and Fr numbers. The recirculation pump speed was varied to control the velocity of the slug. Buoyancy was varied by changing the temperature of the reactor coolant while maintaining the slug at city water temperature.

Two hundred sixty-five thermocouples (TCs) were installed in the downcomer and lower plenum. Eleven levels were monitored—eight in the downcomer and three in the lower plenum. Figure 6 shows the location of thermocouples for the most heavily instrumented levels in the downcomer. At the most instrumented downcomer levels, TCs were positioned every 15 degrees in the middle of the annulus. Every 30 degrees these thermocouples were augmented by two more thermocouples located at different radial positions. These extra thermocouples were used to examine the radial variation of the slug temperature in the downcomer. The outer TC was located at a radial position of 23.5 cm (0.6 cm from the vessel wall), while the inner TC was located at 21.5 cm (0.6 cm from the core barrel). In the less instrumented levels, TCs were spaced 30 degrees apart azimuthally (as indicated by the red dots in the figure). In the lower plenum, there were two rings at 16.5 and 8.25 cm, respectively, and two TCs in the center removed 2 cm from the vertical axis.

Initial conditions consisted of primary system temperatures supplied by downcomer and lower plenum TCs. Boundary conditions consisted of the flowrate and the temperature of fluid entering the simulation boundary through the flange that connects CL A1 to the reactor vessel. The flowrates were determined from either injection tank level (through a differential pressure transducer), or measured directly with an ultrasound flowmeter (calibrated for cold leg geometry and water temperature). Core pressure drops, also measured with differential pressure transducers, completed the definition of boundary conditions.

Data monitored during each test was limited by the data acquisition system (DAS), which could only accommodate 172 channels. Redundant tests were carried out to monitor either downcomer or lower plenum behavior; control levels were acquired during all tests to ensure redundancy. At DAS maximum capacity, the frequency of acquisition was approximately 2 Hz.

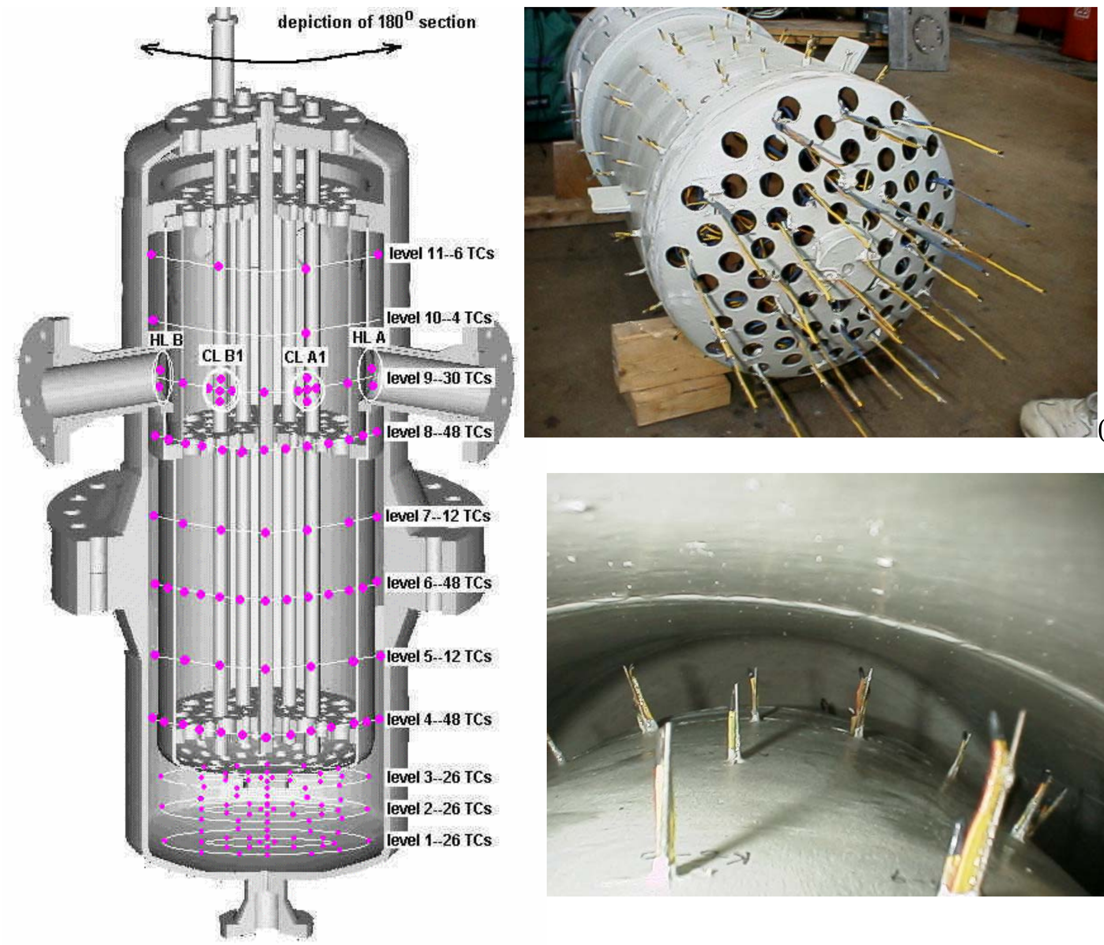

(a)

(b)

Figure 2. Thermocouple locations in the simulation volume with (a) mountings on the core barrel and (b) final position within the downcomer.

One of the most important accommodations for CFD validation was the construction and operations of a visualization facility that provided insights into flow structures that cannot be investigated in a stainless steel facility. The visualization facility was constructed from Plexiglas and had identical cold leg and vessel dimensions for the entire simulation region. Because mixing in the core region was beyond the scope of ISP 43, the visualization facility had an atypical core region and allowed the flow to empty downwards as shown in Figure 4.

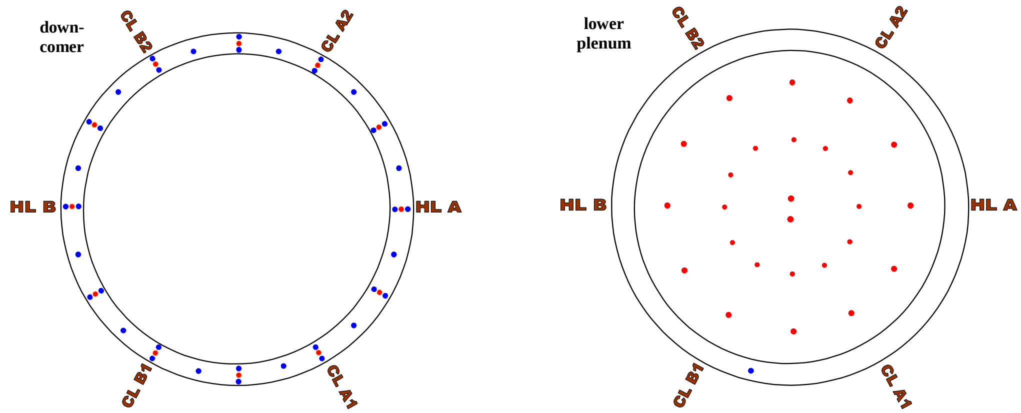

Figure 3. Schematics of downcomer (level 4) and lower plenum (level 2) TC arrangements.

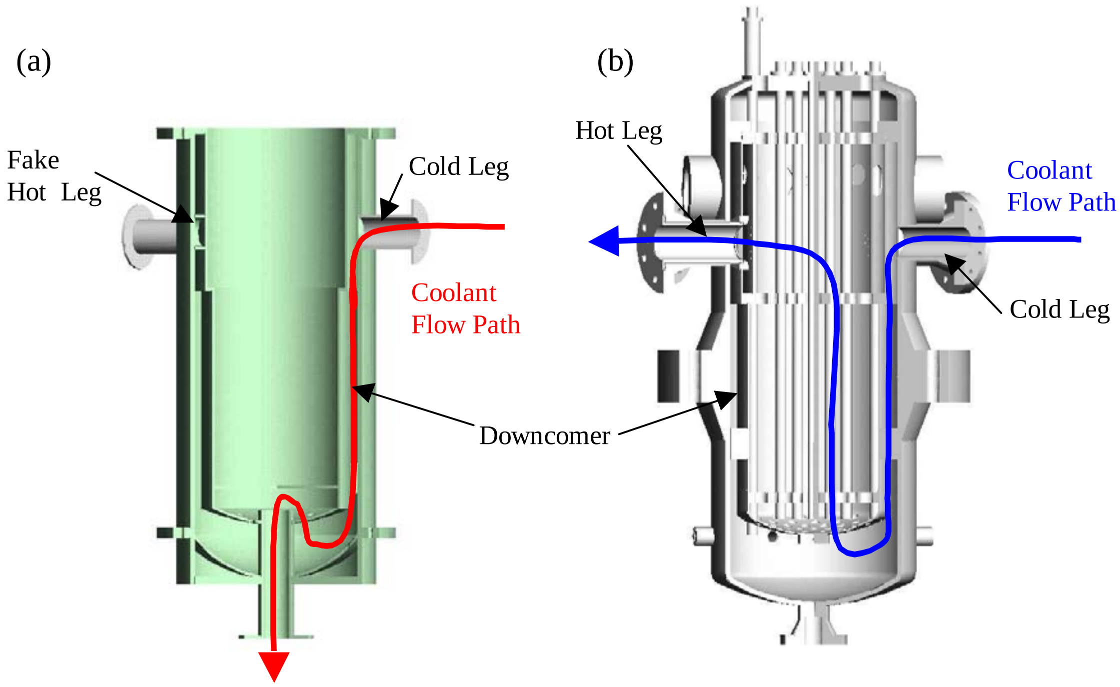

Figure 4. Flow pattern in the visualization facility (a) and the 2x4 Loop (b)

Another measure taken specifically to accommodate CFD computations was the installation of a flow-straightener in the injection cold leg to minimize the azimuthal velocity component as the flow enters the downcomer. The flow-straightener, shown in Figure 5, consisted of a honeycomb structure that occupied the entire flow area of the cold leg. The honeycomb was made of 15 cm long, 6 mm in diameter straws and a thin mesh screen at the straw outlet side. The screen had 8 threads per cm and an open area of 41%. The streamlining achieved by the flow-straightener was tested in the visualization facility.

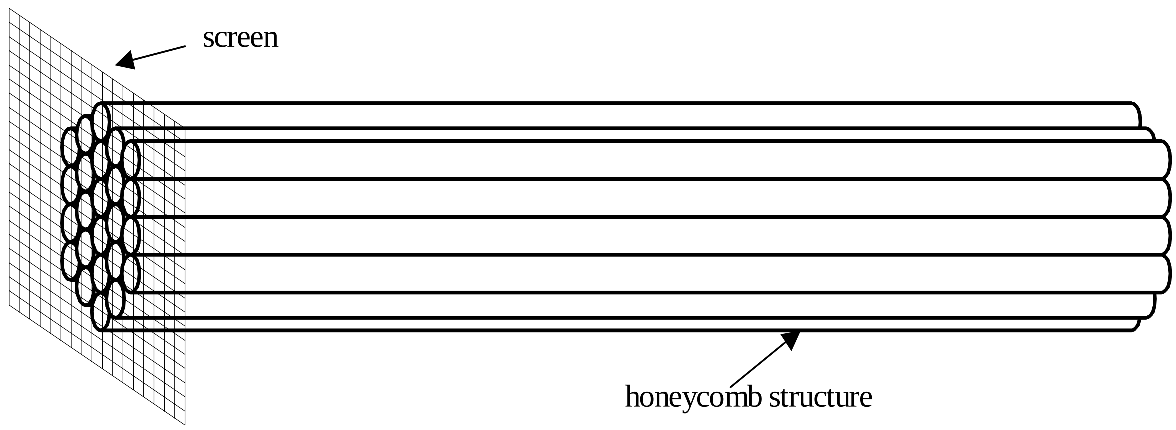

Figure 5. Flow straightener inserted in injection cold leg.

The UM 2x4 Loop was configured to inject a front in test series A and a slug in series B, C and D. In test series A the front was injected from an external tank to minimize the uncertainty in boundary conditions. The entire system, Figure 6, including the external injection tank, was filled with cold (city ambient temperature) water. The primary system was heated with the system heaters. A back-flow preventer stopped the heated water from entering the external tank. Note, however, that water at ambient temperature also flooded the entire cold leg because the external tank is elevated above the vessel. The region of the cold leg downstream of the flow-straightener was mixed with water circulated in the primary system during heat-up. This created a sharp cold-hot interface in the flow-straightener. When the primary system reached a predetermined temperature, the circulation through SG B was stopped and that flow path was isolated. After about one minute—enough time for the primary coolant to come to complete rest—the pump on CL A1 was started. This marked the beginning of the test. The test ended when the 400 l tank emptied.

The participating regions of the loop for test series B are shown in Figure 7. The series build on series A and brought experiments closer to reality: an actual slug was used. The slug was conditioned separately in the slug injection tank, i.e., it was maintained at about 60°C below the primary system temperature. The primary system was heated to about 75°C using the system heaters and recirculating through CL A1 and HL A. When the primary reached the target temperature, the recirculation was stopped and the slug was injected into the lower region of steam generator A. The amount of injected slug was monitored two ways: from the slug injection tank level and thermocouples inserted in the CL A1 riser. The injection was done within about eight minutes, which optimized a time during which the stagnant primary system cannot stratify and an injection rate that did not disturb the hot/cold interface. When the slug reached the pump impeller, the slug injection was stopped and the tank was isolated from the primary system. The overflow that permits the injection of the slug was also isolated. The participating regions formed a closed circuit. Test series C and D were very similar to test series B, and involved the participation of an increasing number of cold legs.

Data and Simulations

The initial figure of merit selected at the first ISP 43 workshop was the average temperature at level 4, i.e., at the exit of the downcomer. During the second workshop, participants selected an additional set of indicators to aid in the overall evaluation of code performance. Specifically, the level average temperature was supplemented with the standard deviation at that level, and the minimum and maximum, which are indicative of the azimuthal mixing of the front/slug. Furthermore, the same first order (level average temperature) information was to be evaluated just below and above the slug entrance, i.e., at levels 8 and 10. The azimuthal distribution figures of merit are also evaluated at these levels.

The simulation boundary was also discussed and agreed upon during the first workshop. The simulation boundary shown in Figure 8 was selected to minimize computational expenditure while meeting the intent of validating the code for mixing in the regions deemed most significant to RBD transients. The simulation started in the injection cold leg at the end of the flow-straightener and ended once the flow penetrated the fuel array.

The nominal test initial and boundary conditions supplied to ISP 43 participants were taken from the second of the 18 redundant 93% pump speed 60 ºC primary to front temperature difference. The initial primary coolant temperature was specified to be uniform at 74 °C. The initial and boundary conditions for every test series consisted of flow rate and temperature of the injected front/slug. In addition, because the simulation boundary is limited, the pressure drop had to be externally supplied. A differential pressure probe measured the core pressure drop with terminals at the core inlet level and the hot leg A entrance. Figure 9 and Figure 10 illustrate the boundary conditions supplied for test series A.

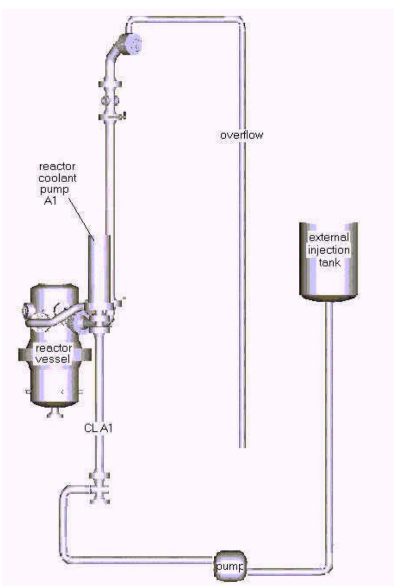

Figure 6. UM 2x4 Loop configuration for test series A—note that only participating components are shown.

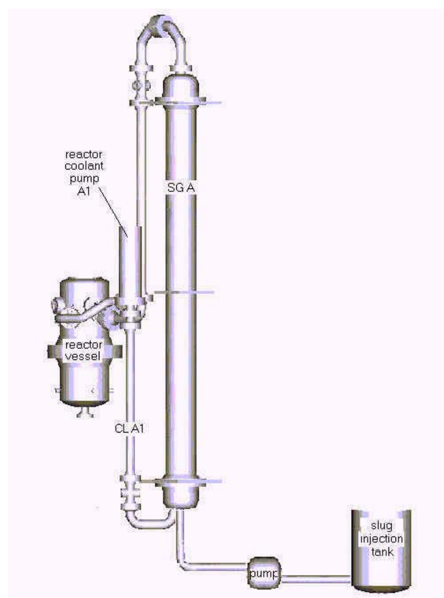

Figure 7. UM 2x4 Loop configuration for test series B—note that only participating components are shown.

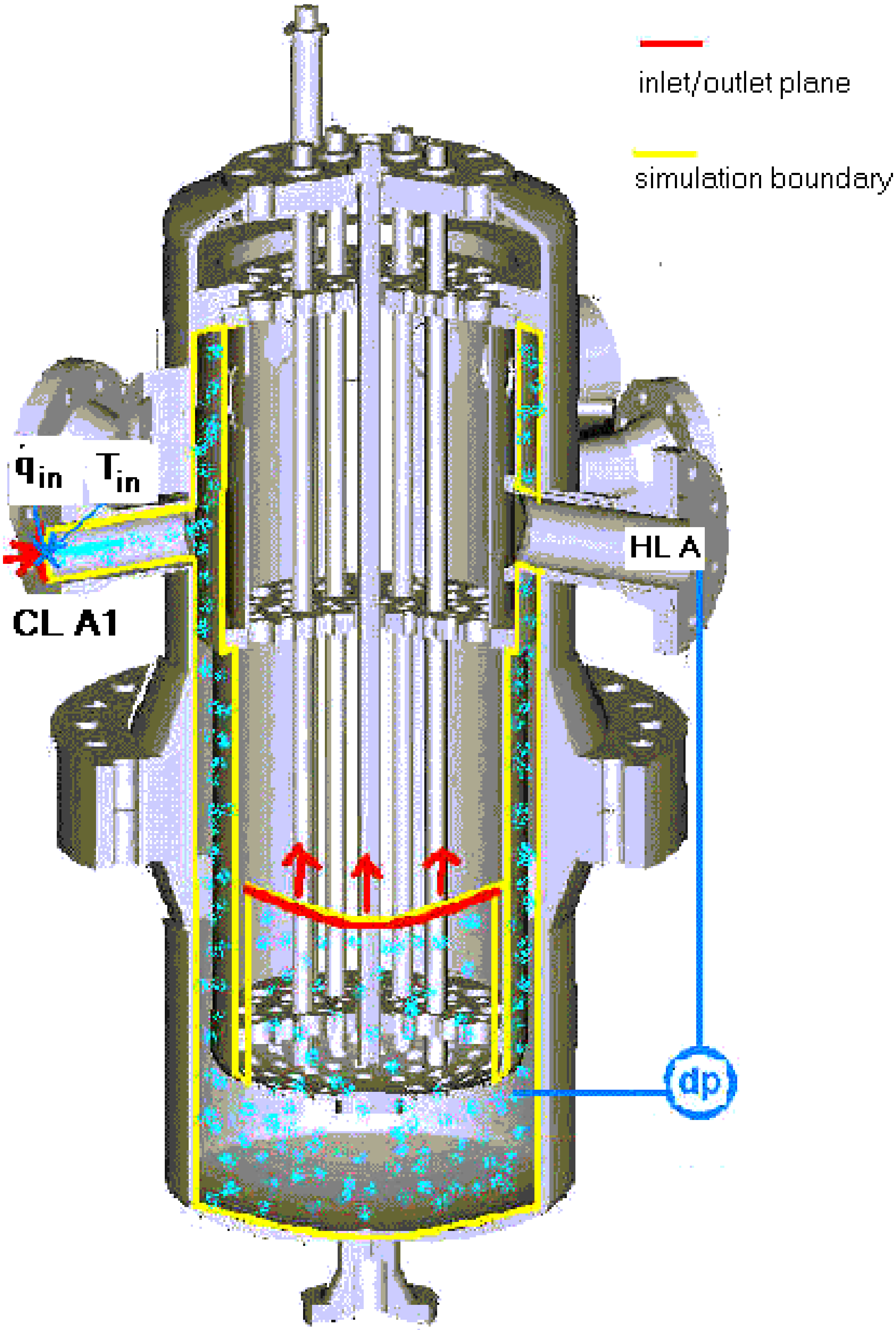

Figure 8. The recommended simulation boundary for ISP Nr. 43

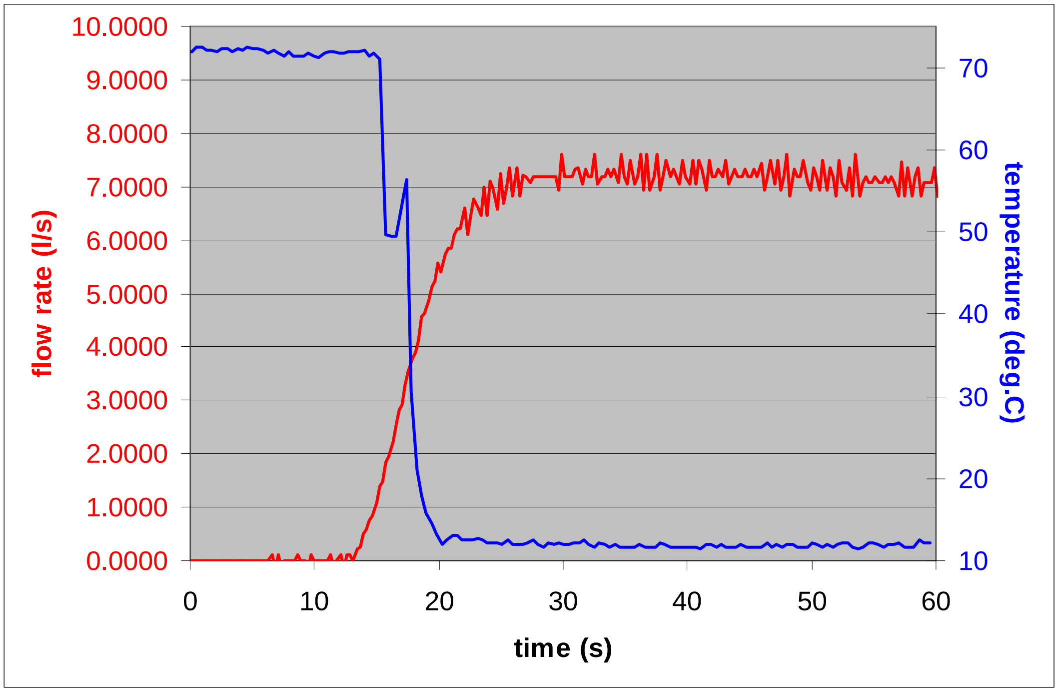

Figure 9. Flow and temperature boundary conditions for test A

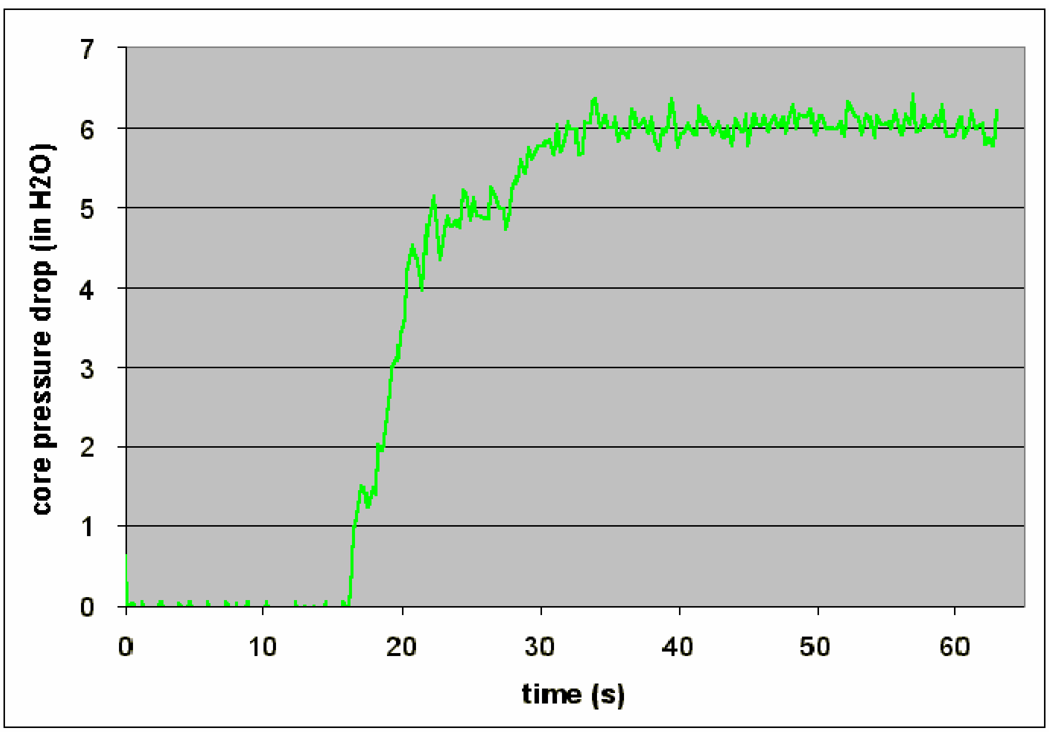

Figure 10. Core pressure drop boundary conditions for test A

For test series A an experimental uncertainty band was obtained by running 18 redundant tests. Even though running redundant tests can substantially increase the experimental burden, it is highly desirable that plots comparing CFD results and experimental data should include a visual display of the error bars on the experimental data. Only 16 series A tests were used because of atypicalities identified in two of the tests. Six redundant tests were collected for test series B. Test series C and D used only two tests each where the second was collected solely as a confirmatory test. Generating an experimental uncertainty band is essential, especially in complex tests were substantial uncertainties are to be expected. In tests series A, the importance of redundant tests was further demonstrated by observing the effect of boundary conditions on flow pattern and consequently on code simulations. The effect of Froude number on flow pattern will be addressed at the end of this section.

Figure 11 plots the azimuthally-averaged temperature histories at level 4. Experimental and computational data are shown. The solid black line and the black error bars represent the loop data for the 16 redundant tests. The nominal test, i.e., the test for which boundary conditions where supplied to participants, falls within the standard deviation and is represented through a thin black line. The red line and the red error bars represent the ensemble average and standard deviation of the 8 redundant visualization tests. The 2x4 Loop and visualization facility temperature histories are with each other's standard deviation. Participant submissions are indicated by the other lines on the plot. While computations appear to be generally in very good agreement, a general trend of slight under mixing is noticeable in about half of the simulations. This under-mixing is also noticeable in the standard deviation of temperatures at level 4 as plotted in Figure 11.

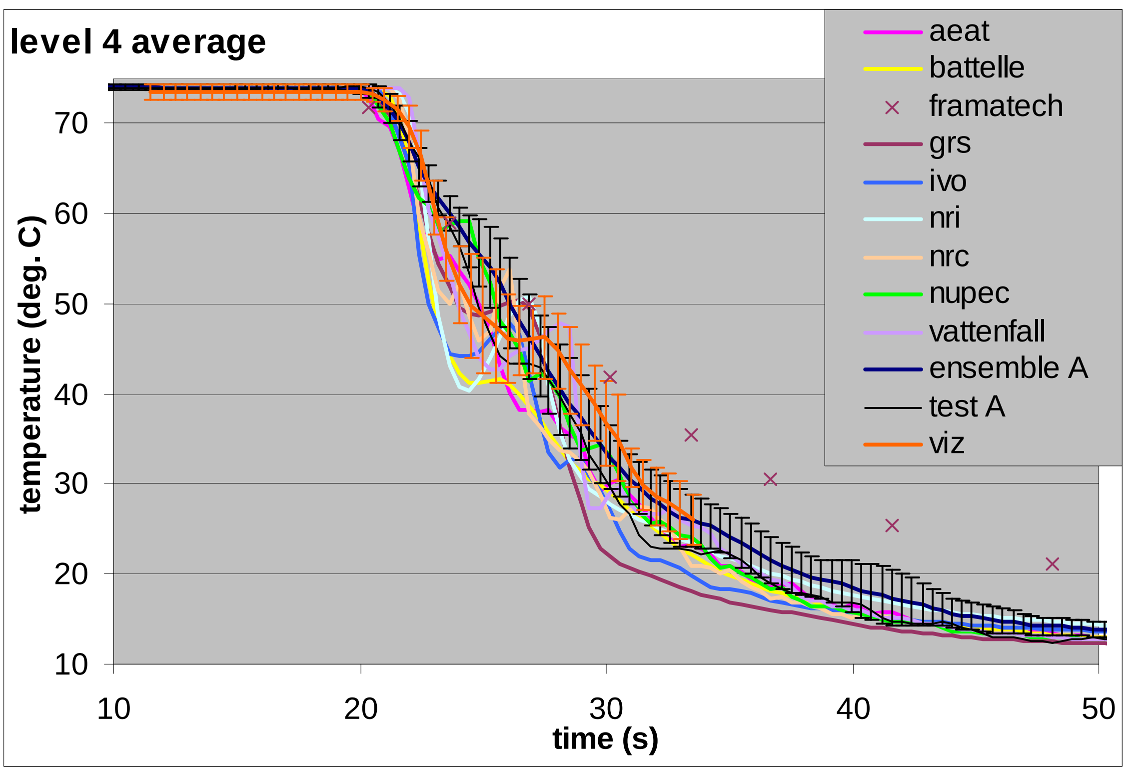

Figure 11. Level 4 azimuthally-averaged temperature histories

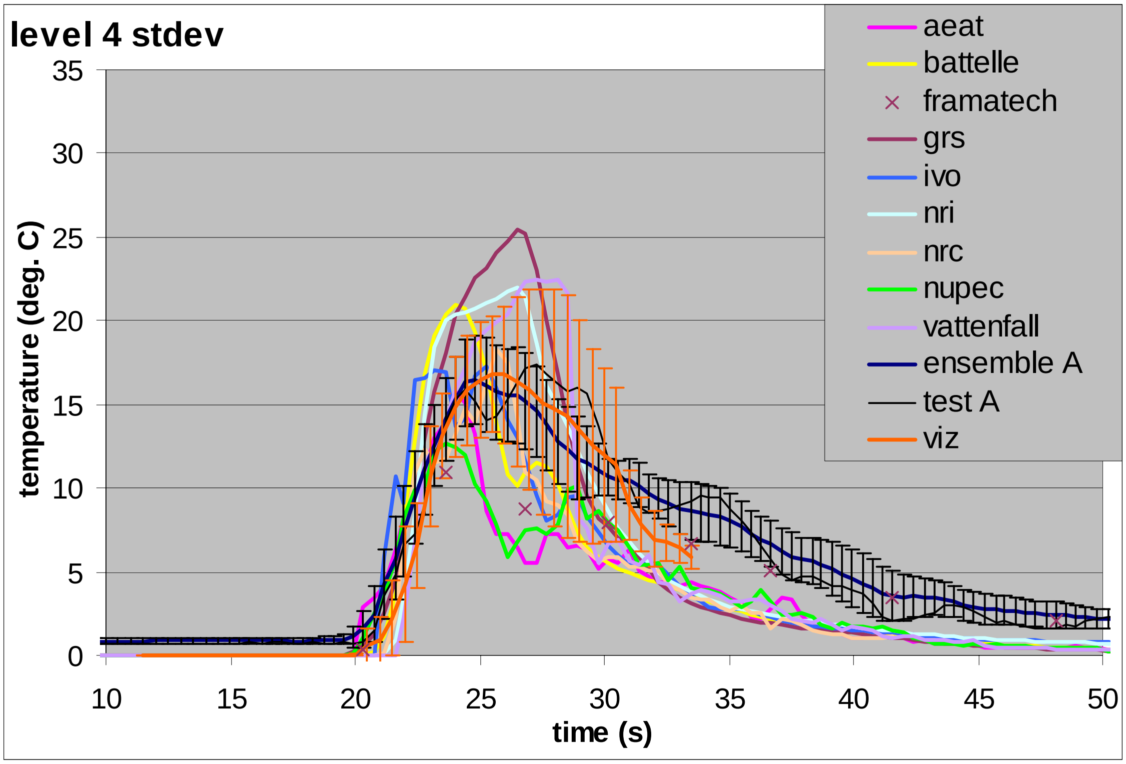

Figure 12. History of the standard deviation of the 24 channel-center thermocouples at level 4

Details of test series A and B are contained in the ISP 43 final report published by OECD/CSNI and will not be repeated here. [2] The mixing characteristics of test series C and D were fully consistent with test series B. Figure 13 shows the average mixing at level 4 for all the integral-effect type test series. The three trends in each plot correspond to temperature differences between the primary coolant and the slug of 4.4, 10 and 15.6°C, respectively. Like the data for test series A and B, the data for test series C and D is part of the U.S. NRC databank. Woods [3] discusses the experimental findings of the last two test series.

One of the most significant findings of ISP 43 was that acquiring redundant data should be compulsory especially for complex separate effect and integral tests. This is not surprising given the expectation of large uncertainties associated with such tests. In the case of the RBD transient tests at the UM 2x4 Loop, it was noted the 16 redundant series A tests had different flow patterns. The bulk figure of merit, the average dilution at level 4 was not affected by the change in flow pattern. However, some tests showed that, upon entering the downcomer, the flow would go straight downward along a single branch. Yet other "redundant" tests showed that the flow that entered the downcomer split into two branches, with one going around the downcomer to the right and the other to the left, leaving a relatively stagnant region under the injection site.

A close examination of the data revealed that a relatively small temperature difference in boundary conditions was enough to cause the change in flow pattern. Because the difference was

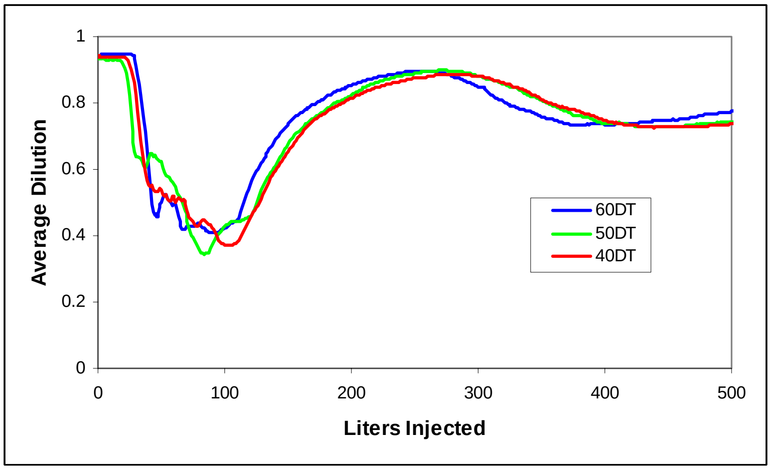

(a) test series B

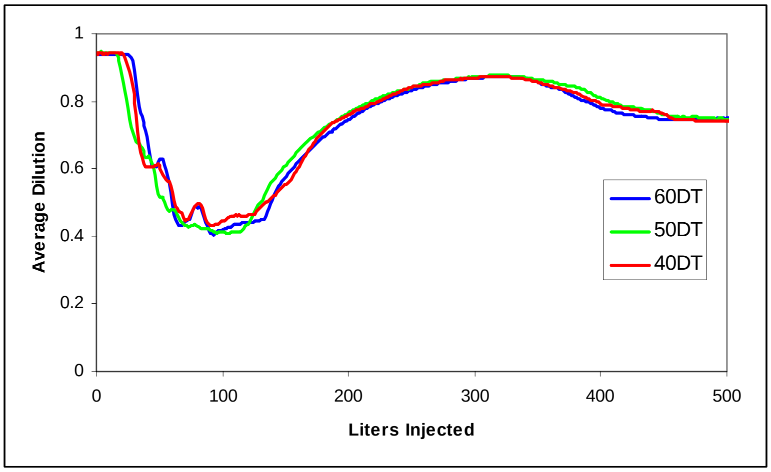

(b) test series C

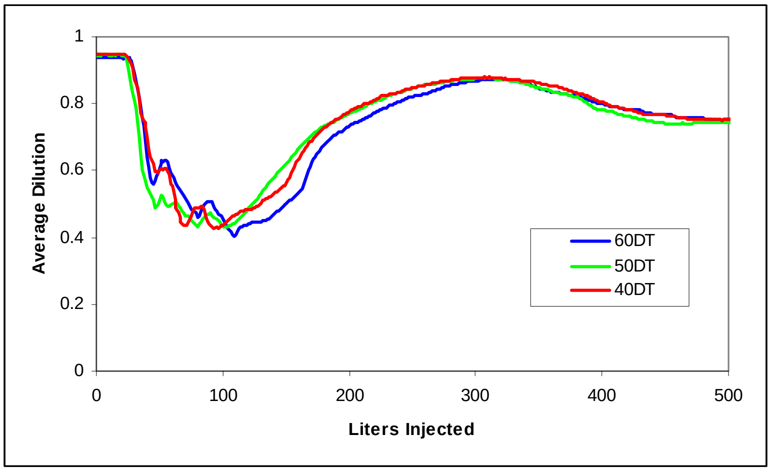

(c) test series D

Figure 13. Average dilution at level 4 for 40% recirculation pump speed for test series B, C and D

affecting buoyancy, the Froude number history was calculated for each of the "redundant" tests. The following Fr number relationship was used:

$$Fr = \frac{V}{\left[gD\beta(T_a)(T_0 - T_a)\right]^{0.5}},$$

where: V is the jet exit velocity (cold leg)
D is the jet exit diameter
g is gravitational force constant
T_0 is the jet exit temperature (injection of a front NOT a slug)
T_a is the ambient temperature (primary coolant temperature), and
$\beta(T_a)$ is the thermal expansion coefficient of water at ambient temperature.

The resulting Fr number histories plotted in Figure 14 showed unambiguously the impact of a relatively small variation in slug-coolant temperature difference on the flow pattern.

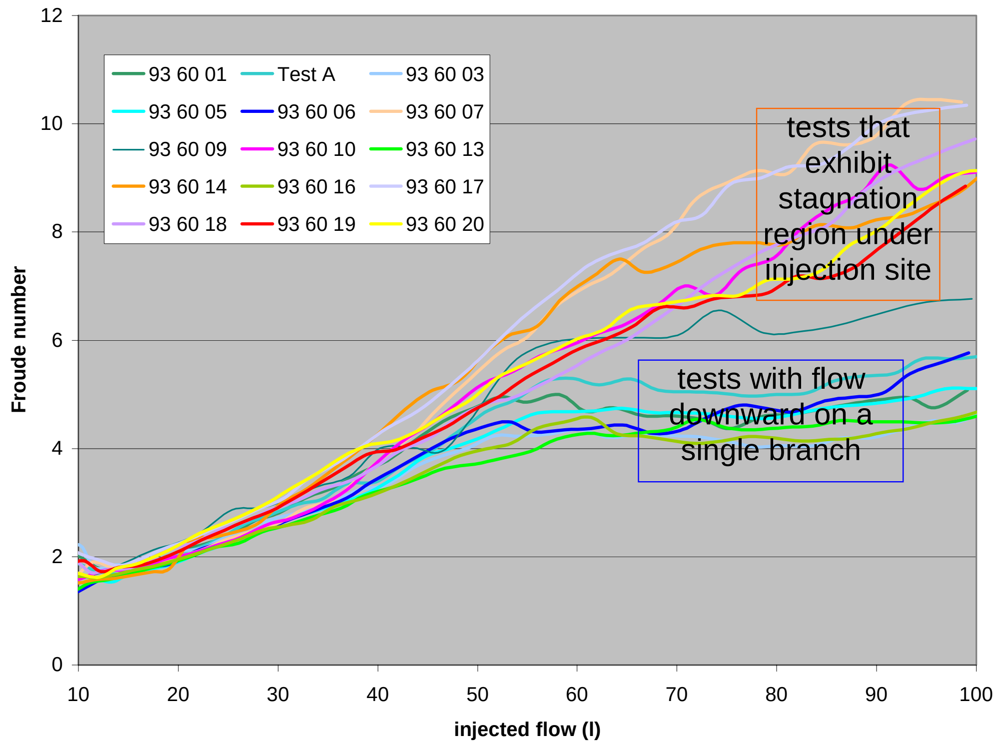

Figure 14. Froude number histories for the redundant tests of series A

These findings were confirmed by examining the downcomer pattern over the broad range of conditions from all test series. The examination showed that a Fr threshold value of about 6-7 exists where the flow pattern changes from a single downward branch to two branches that surround the downcomer. Figure 15 and Figure 16 show the pattern in the unfolded downcomer for single and double branch flows. Figure 17 shows the downcomer flow pattern from participant submissions. Not surprisingly, some exhibit the single branch behavior while others show flow along two branches.

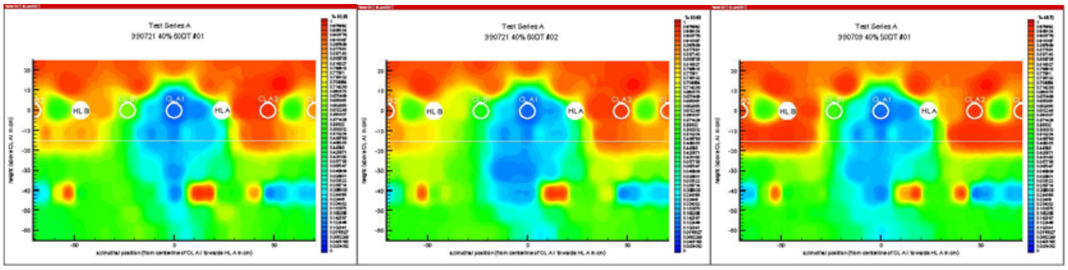

40% 60DT Fr = 3.93 | **40% 60DT Fr = 3.97** | **40% 50DT Fr = 4.31**

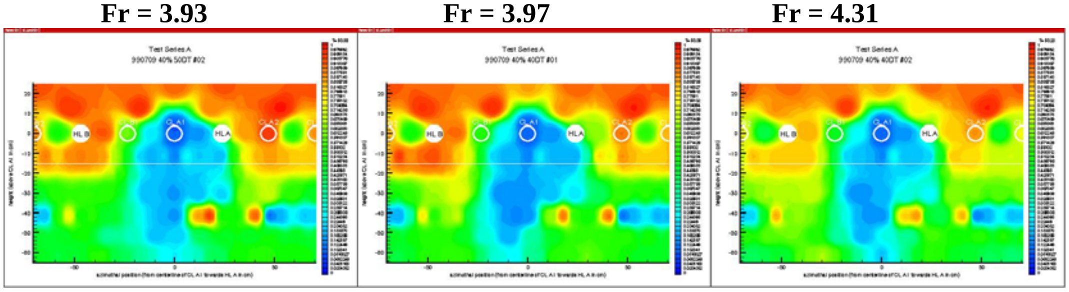

40% 50DT Fr = 4.39 | **40% 40DT Fr = 4.86** | **40% 40DT Fr = 5.21**

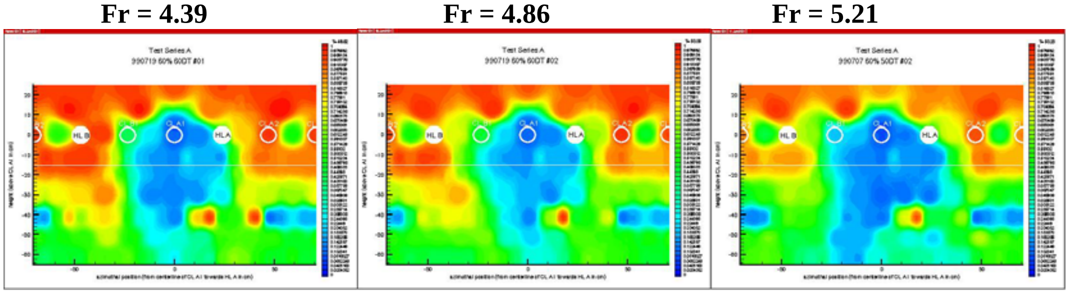

60% 60DT Fr = 5.35 | **60% 60DT Fr = 5.45** | **60% 50DT Fr = 6.30**

Figure 15. Flow patterns for series A tests with Fr ranging from 4.4 to 6.3

Conclusions

The success of ISP 43 is in large part due to the close collaboration between experimentalists and code analysts. This collaboration was essential in setting the most meaningful figures of merit. Another important contributor to the success of ISP 43 was the use of a CFD code by experimentalists. The code was used to scope out the placement of instrumentation. It was also used to run the blind and open test simulations at the same time as the participants. This facilitated debugging input models and ensured data sufficiency.

The most important lesson learned is the importance of establishing an experimental uncertainty band. This is especially important in integral testing were boundary and initial conditions cannot be tightly controlled. In ISP 43, the redundant tests showed the existence of two flow patterns in what was thought to be redundant tests. The effect of Fr number on flow pattern was an unanticipated experimental finding.

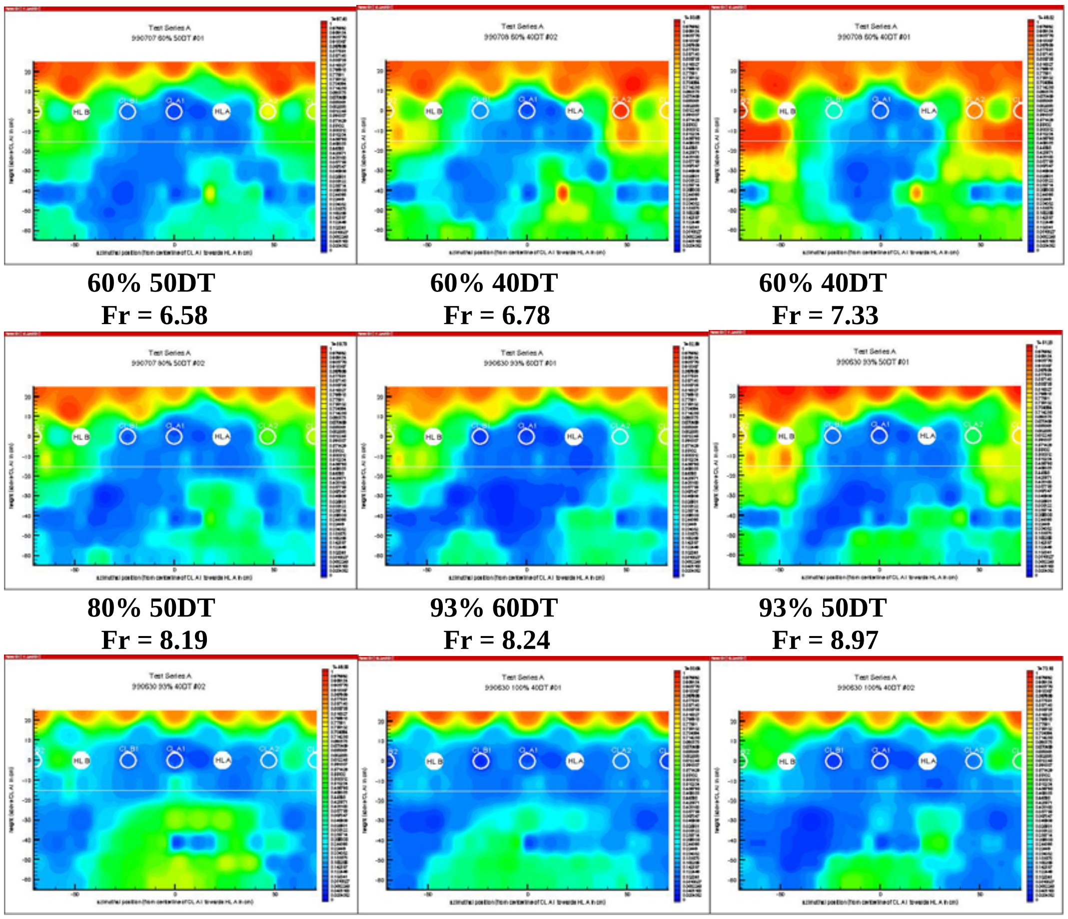

60% 50DT
Fr = 6.58

60% 40DT
Fr = 6.78

60% 40DT
Fr = 7.33

80% 50DT
Fr = 8.19

93% 60DT
Fr = 8.24

93% 50DT
Fr = 8.97

93% 40DT
Fr = 10.96

100% 40DT
Fr = 11.69

100% 40DT
Fr = 11.82

Figure 16. Flow patterns for series A tests with Fr ranging from 6.6 to 11.8

References

[1] AIAA G-077-1998, AIAA Guide for the Verification and Validation of Computational Fluid Dynamics Simulations, *AIAA Standards Series*

[2] NEA/CSNI/R(2000)22, ISP-43: Rapid Boron Dilution Transient Experiment, Comparison Report, OECD/CSNI Report

[3] Woods, B., "Boron-dilution Experiments at the University of Maryland 2x4 Loop Facility," Ph.D. thesis, University of Maryland, 2001

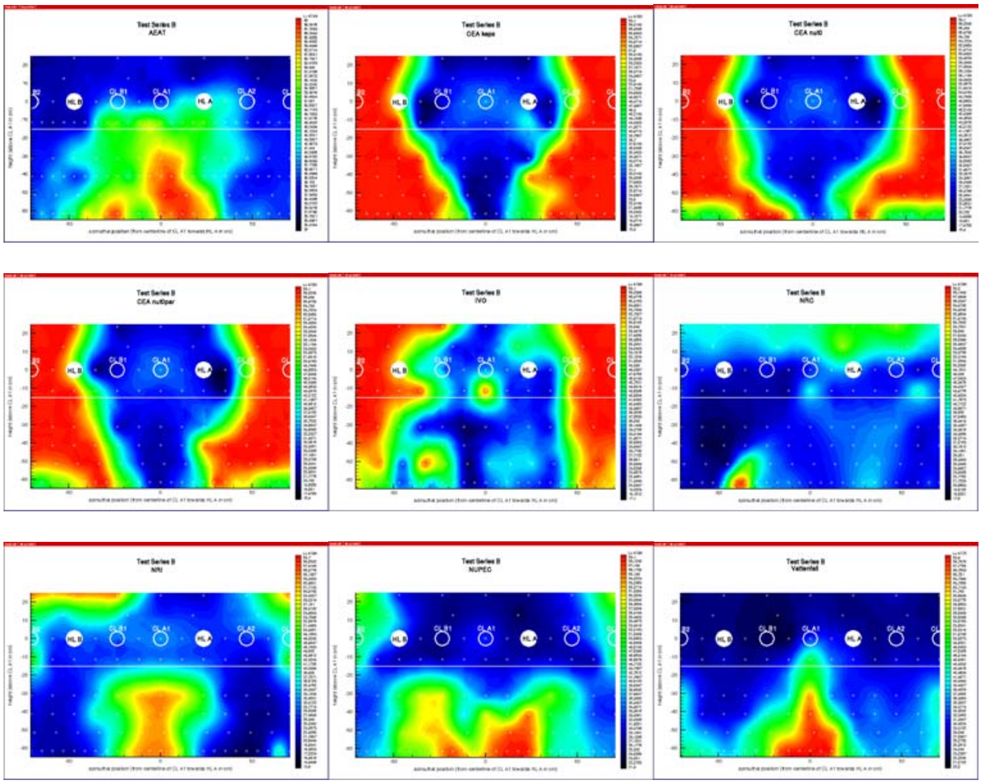

Figure 17. Downcomer flow pattern from participant submissions